BMB Reports - Manuscript Submission

Manuscript Draft

Manuscript Number: BMB-21-148

Title: Downregulation of JMJD2a and LSD1 is involved in CK2 inhibition-mediated cellular senescence through the p53-SUV39h1 pathway

Article Type: Article

Keywords: CK2; JMJD2a; LSD1; senescence-associated heterochromatin foci; p53

Corresponding Author: Young-Seuk Bae

Authors: Jeong-Woo Park[1], Young-Seuk Bae[1,*]

Institution: [1]School of Life Sciences, BK21 FOUR KNU Creative BioResearch Group, Kyungpook National University,

Downregulation of JMJD2a and LSD1 is involved in CK2 inhibition-mediated cellular senescence through the p53–SUV39h1 pathway

Jeong-Woo Park[1] and Young-Seuk Bae[1,*]

[1]School of Life Sciences, BK21 FOUR KNU Creative BioResearch Group, Kyungpook National University, Daegu 41566, Republic of Korea

[*]Corresponding author. Tel: 82-53-950-6355; E-mail: ysbae@knu.ac.kr

Running title: CK2-mediated SAHF regulation via JMJD2a and LSD1

ABSTRACT

Lysine methylation is one of the most important histone modifications that modulate chromatin structure. In the present study, the roles of the histone lysine demethylases JMJD2a and LSD1 in CK2 downregulation-mediated senescence were investigated. The ectopic expression of JMJD2a and LSD1 suppressed the induction of senescence-associated β-galactosidase activity and heterochromatin foci formation as well as the reduction of colony-forming and cell migration ability mediated by CK2 knockdown. CK2 downregulation inhibited JMJD2a and LSD1 expression by activating the mammalian target of rapamycin (mTOR)–ribosomal p70 S6 kinase (p70S6K) pathway. In addition, the downregulation of JMJD2a and LSD1 was involved in activating the p53–$p21^{Cip1/WAF1}$–SUV39h1–trimethylation of the histone H3 Lys9 (H3K9me3) pathway in CK2-downregulated cells. Further, CK2 downregulation-mediated JMJD2a and LSD1 reduction was found to stimulate the dimethylation of Lys370 on p53 (p53K370me2) and nuclear import of SUV39h1. Therefore, this study indicated that CK2 downregulation reduces JMJD2a and LSD1 expression by activating mTOR, resulting in H3K9me3 induction by increasing the p53K370me2-dependent nuclear import of SUV39h1. These results suggest that CK2 is a potential therapeutic target for age-related diseases.

Key Words: CK2; JMJD2a; LSD1; senescence-associated heterochromatin foci; p53

INTRODUCTION

Cellular senescence, which is characterized by an irreversible arrest of the cell cycle, is triggered by telomere attrition and various genotoxic stressors, all of which ultimately

activate DNA damage responses (1, 2). Senescent cells exhibit specific markers; these include increased senescence-associated β-galactosidase (SA-β-gal) activity, activation of the p53–$p21^{Cip1/WAF1}$ pathway, and formation of senescence-associated heterochromatin foci (SAHF), which result from the condensation of chromatin into punctate heterochromatic domains (3, 4). The formation of SAHF suppresses the expression of genes encoding cell cycle progression-associated proteins, including cyclin A and cyclin D1. SAHF include several markers, such as the trimethylation of histone H3 Lys9 (H3K9me3) and binding of heterochromatin protein 1 (HP1α, β, and γ) to H3K9me3 (5).

H3K9 methylation is mediated by histone lysine methyltransferases, including SUV39h1, G9a, and GLP (6, 7). By contrast, histone lysine demethylases, including the JmjC domain-containing histone demethylase (JMJD2/KDM4) and lysine-specific demethylase 1 (LSD1/KDM1a), remove methyl groups from H3K9 (8-11). The JMJD2 subfamily (JMJD2a, b, c, and d) catalyzes the specific removal of di- and trimethyl groups from H3K9. LSD1 specifically demethylates H3K9 (either mono- or dimethylated). JMJD2a and JMJD2c cooperate with LSD1 to regulate protein lysine methylation (12). The overexpression of H3K9 demethylases is implicated in various cancer types, including prostate, bladder, and breast cancer (13). LSD1 can also target nonhistone proteins such as p53 and E2F1 (14, 15). A critical factor in the modulation of p53 activity is the control of p53 protein stability, which is primarily coordinated via post-translational modifications, including phosphorylation, acetylation, methylation, and ubiquitination.

The mammalian target of rapamycin (mTOR) is a protein kinase that controls cell growth in response to nutrients, growth factors, and cellular energy (16). The control of anabolic processes by mTOR involves the processes of transcription, protein synthesis,

ribosome biogenesis, and nutrient transport. The activation of mTOR leads to the phosphorylation of several proteins, including eukaryotic translation initiation factor 4E (eIF4E)-binding proteins (4E-BPs) and ribosomal p70 S6 kinase (p70S6K), via which mTORC1 controls protein synthesis (17).

Our previous studies revealed that CK2 downregulation accelerated senescence via the p53–p21$^{Cip1/WAF1}$ pathway in human cells and that p53 increased after reactive oxygen species production via the PI3K–AKT–mTOR pathway (18-20). The *Caenorhabditis elegans* ortholog of CK2β (*kin-10*) knockdown induces the expression of age-related biomarkers, including the reduced longevity and retardation of locomotion in *C. elegans* (21). Also, CK2 downregulation induces H3K9me3 and SAHF formation by upregulating SUV39h1 expression in a p53-dependent manner (22). Therefore, these findings suggest that H3K9 demethylases are downregulated during CK2 downregulation-mediated senescence.

In this study, we investigated the roles of JMJD2a and LSD1 in the formation of SAHF after CK2 downregulation in HCT116 and MCF-7 cells. The results showed that JMJD2a and LSD1 overexpression successfully abrogated CK2 downregulation-induced senescence and that CK2 knockdown inhibited JMJD2a and LSD1 mRNA translation, thereby increasing p53 K370 methylation. This could lead to the activation of the p53–SUV39h1–H3K9me3 pathway. Of note, this is the first study to show that CK2 can regulate histone demethylases. As CK2 is associated with senescence and aging, it is be a potential therapeutic target for age-related diseases.

RESULTS

Ectopic expression of JMJD2a and LSD1 suppressed the induction of SA-β-gal activity and SAHF formation as well as the reduction of colony-forming and cell migration ability mediated by CK2 knockdown

We have previously shown that CK2 downregulation could induce SAHF formation and H3K9me3 by increasing H3K9 trimethyltransferase SUV39h1 expression in both HCT116 and MCF-7 cells (21). To determine the role of H3K9 demethylases in CK2 knockdown-induced senescence, MCF-7 and HCT116 cells were treated with either pCMV-JMJD2a or pCMV-LSD1 in the presence of CK2α siRNA. Consistent with a previous study (18), CK2 downregulation stimulated the SA-β-gal activity. However, the ectopic expression of JMJD2a and LSD1 significantly suppressed the induction of the SA-β-gal activity in CK2-knockdown cells (Fig. 1A). SAHF contain various markers of transcriptionally silent heterochromatin, including H3K9me3 and HP1γ (3, 4). Therefore, SAHF formation was detected via 4′,6-diamidino-2-phenylindole (DAPI) staining and immunofluorescence analysis using antibodies against H3K9me3 and HP1γ. CK2 downregulation increased the fluorescence intensity of H3K9me3 (red) and its co-localization with HP1γ (green) in DAPI-dense heterochromatin foci (blue), and the ectopic expression of JMJD2a and LSD1 suppressed the induction of SAHF formation in CK2-knockdown cells (Fig. 1B). Cell colony formation and migration abilities are critical processes in cancer tumorigenesis and metastasis (23). As senescence suppresses tumor progression (1), colony formation and cell migration assays were performed, and the results showed that CK2 downregulation inhibited colony formation and cell migration abilities. However, the ectopic expression of JMJD2a and LSD1 suppressed this reduction of colony formation and cell migration abilities mediated by CK2 knockdown (Supplementary Fig. 1). These results suggest that JMJD2a and LSD1

downregulation is required for CK2 downregulation-induced senescence markers, including increased SA-β-gal staining and SAHF formation and decreased colony formation and cell migration abilities.

CK2 downregulation inhibited the expression of JMJD2a and LSD1 at the translational level by activating the mTOR–p70S6K pathway

Next, we investigated whether CK2 regulates H3K9 demethylase expression in cells. Treating MCF-7 and HCT116 cells with CK2α siRNA reduced the protein levels of H3K9 demethylases (JMJD2a, JMJD2c, and LSD1) compared with control cells. By contrast, treatment with pcDNA3.1-HA-CK2α increased the protein levels of JMJD2a, JMJD2c, and LSD1, suggesting that CK2 may positively regulate the expression of these H3K9 demethylases (Fig. 2A). As CK2 knockdown-mediated senescence is p53-dependent (19), the effect of p53 on the expression of these demethylases was examined. Similar to cells containing wild-type p53, the protein levels of these demethylases were decreased by CK2α knockdown and increased by CK2α overexpression in both HCT116 $p53^{-/-}$ cells and MDA-MB-435 cells (which contained a point mutation within p53), suggesting that p53 is not involved in the CK2-mediated regulation of these demethylases (Supplementary Fig. 2). We next examined whether the decrease in the protein levels of these demethylases is correlated with a decrease at the transcriptional level. The knockdown or overexpression of CK2α did not affect the mRNA levels of JMJD2a, JMJD2c, and LSD1, suggesting that CK2 regulates the expression of these demethylases at the post-transcriptional level (Supplementary Fig. 3). Further, to investigate whether CK2 regulates the expression of these demethylases at the translation step, cells transfected with CK2α siRNA were cultured in the presence of the

protein synthesis inhibitor cycloheximide (50 μg/ml). The protein levels of JMJD2a, JMJD2c, and LSD1 were decreased steadily after 4–16 h of cycloheximide treatment, suggesting that CK2 downregulation reduces JMJD2a, JMJD2c, and LSD1 expression at the translational step (Fig. 2B). As the mTOR–p70S6K axis is associated with protein synthesis (17), cells were treated with CK2α siRNA in the presence of the mTOR inhibitor rapamycin (100 nM). The mTOR–p70S6K pathway activation was then measured by monitoring the phosphorylation of mTOR and its downstream target p70S6K. The results revealed that CK2 downregulation markedly increased the levels of phospho-mTOR (S2448) and phospho-p70S6K (T389). However, rapamycin treatment attenuated both the activation of mTOR–p70S6K and reduction of demethylases in CK2-downregulated cells (Fig. 2C). Taken together, these results suggest that CK2 downregulation decreases JMJD2a, JMJD2c, and LSD1 expression at the translational level via the activation of the mTOR–p70S6K pathway.

CK2 downregulation-mediated reduction of JMJD2a and LSD1 activated the p53–p21$^{Cip1/WAF1}$– SUV39h1–H3K9me3 axis

We then transfected cells with pCMV-JMJD2a or pCMV-LSD1 in the presence of CK2α siRNA to investigate the roles of JMJD2a and LSD1 in H3K9me3 and SUV39h1 expression induced by CK2 downregulation. Consistent with a previous study (22), CK2α downregulation increased the levels of H3K9me3 and expression of SUV39h1. However, JMJD2a and LSD1 overexpression abrogated the induction of H3K9me3 and SUV39h1 in CK2-downregulated cells (Fig. 3A). As the p53–p21$^{Cip1/WAF1}$ pathway is an upstream activator of CK2 downregulation-mediated H3K9me3 and SUV39h1 expression (24), the effect of JMJD2a and LSD1 on the expression of p53 and p21$^{Cip1/WAF1}$ was also evaluated.

The overexpression of JMJD2a and LSD1 suppressed the induction of p53 and $p21^{Cip1/WAF1}$ in CK2-downregulated cells (Fig. 3A). By contrast, CK2α overexpression decreased the levels of p53, $p21^{Cip1/WAF1}$, SUV39h1, and H3K9me3. Moreover, the knockdown of JMJD2a and LSD1 attenuated the reduction of p53, $p21^{Cip1/WAF1}$, SUV39h1, and H3K9me3 in CK2α-overexpressing cells (Fig. 3B). To examine the effect of JMJD2a and LSD1 on the transcriptional activity of p53, we performed chromatin immunoprecipitation assay with p53 antibody. The results showed that CK2 knockdown reduced p53 binding to the $p21^{Cip1/WAF1}$ promoter, whereas the overexpression of JMJD2a and LSD1 suppressed the CK2 knockdown-mediated reduction of p53 binding to the $p21^{Cip1/WAF1}$ promoter (Supplementary Fig. 4). The CK2-downregulated and JMJD2a/LSD1-upregulated cells were further treated with p53 cDNA to confirm the role of p53 in the reduction of SUV39h1, which was mediated by the ectopic expression of JMJD2a or LSD1 in CK2-downregulated cells. The induced p53 overexpression rescued the reduction of SUV39h1 that was mediated by the overexpression of either JMJD2a or LSD1. However, p53 overexpression did not affect JMJD2a and LSD1 levels, indicating that p53 is an upstream regulator of SUV39h1 but not JMJD2a and LSD1 (Supplementary Fig. 5). Taken together, these results suggest that the downregulation of JMJD2a and LSD1 in CK2-downregulated cells activates the p53–$p21^{Cip1/WAF1}$ pathway, leading to the expression of SUV39h1 and H3K9me3.

CK2 downregulation-mediated JMJD2a and LSD1 reduction stimulated the dimethylation of p53 Lys370 and led to the nuclear import of SUV39h1

We previously reported that CK2 downregulation enhances the nuclear import and subsequent stabilization of SUV39h1 by inhibiting the interaction between p53 and SUV39h1

(24). Hence, immunoprecipitation analyses were performed to determine whether JMJD2a and LSD1 regulate this interaction between p53 and SUV39h1 in CK2α-downregulated cells. Compared with control cells, a lower amount of SUV39h1 was coprecipitated with p53 in CK2-downregulated cells. However, the ectopic expression of JMJD2a or LSD1 enhanced the coprecipitation of SUV39h1 with p53 in cells (Fig. 4A). By contrast, more SUV39h1 was coprecipitated with p53 in cells with CK2α upregulation than control cells; however, treatment with JMJD2a or LSD1 siRNA abrogated this effect (Fig. 4B). Taken together, these results suggest that the binding of p53 to SUV39h1 is decreased by reducing JMJD2a and LSD1 in CK2-downregulated cells.

LSD1 has been reported to demethylate the dimethyl group of Lys370 on p53 (p53K370me2) (14, 15); however, the role of JMJD2a is still unclear. Our immunoblot analysis using a p53K370me2-specific antibody revealed that p53K370me2 was increased in CK2-downregulated cells and that the ectopic expression of JMJD2a or LSD1 suppressed this effect, indicating that JMJD2a and LSD1 demethylate the dimethyl group of p53K370me2 (Fig. 3A). To examine the effect of p53K370me2 on the nuclear localization of p53 and SUV39h1, the cytoplasm and nuclei were isolated from MCF-7 and HCT116 cells. The accumulation of p53K370me2, total p53, and SUV39h1 was greater in the nuclear extracts than that in the cytosolic extracts of cells with CK2 downregulation. However, the overexpression of JMJD2a or LSD1 suppressed the nuclear transport of SUV39h1 in CK2-downregulated cells, which suggested that JMJD2a and LSD1 negatively regulate the nuclear import of SUV39h1 in CK2-downregulated cells (Fig. 4C). Taken together, these results suggest that the CK2 downregulation-mediated reduction of JMJD2a and LSD1 stimulates

p53K370me2, leading to the decreased interaction between p53 and SUV39h1 and the subsequent nuclear import of SUV39h1.

DISCUSSION

The downregulation of CK2 has been reported to induce the expression of several senescence markers, including p53–p21$^{Cip1/WAF1}$ activation, SA-β-gal staining, and SAHF formation, in human cells (18-22, 24). As JMJD2a and LSD1 accelerate H3K9me3 demethylation, we examined whether these demethylases are associated with CK2 downregulation-mediated SAHF formation. The present study showed that the ectopic expression of either JMJD2a or LSD1 successfully abrogated the induction of CK2 downregulation-mediated senescence markers such as the SA-β-gal activity, p53–p21$^{Cip1/WAF1}$ pathway activation, H3K9me3, and SAHF formation as well as the reduction of colony formation and cell migration abilities in HCT116 and MCF-7 cells. These findings indicate that the downregulation of JMJD2a and LSD1 may be required for the induction of senescence-specific phenotypes in CK2-downregulated cells (Figs. 1 and 3; Supplementary Fig. 1). In accordance, the protein levels of JMJD2a, JMJD2c, and LSD1 were reduced by CK2 downregulation, whereas CK2α overexpression increased their protein levels (Fig. 2A). Moreover, the present study indicated that CK2 downregulation decreased JMJD2a and LSD1 expression at the translational level by activating the mTOR–p70S6K pathway (Fig. 2B and 2C, Supplementary Fig. 3). In our previous study, CK2 downregulation was found to reduce the expression of the H3K9 dimethyltransferases G9a, GLP, and SETDB1 at the transcriptional level and increase the protein stability of the H3K9 trimethyltransferase SUV39h1 at the post-translational level (22). Therefore, our previous and present study findings suggest that CK2 regulates the

expression of various histone-modifying enzymes at different steps; e.g., H3K9 dimethyltransferases (G9a, GLP, and SETDB1) at the transcriptional level, H3K9 demethylases (JMJD2a, JMJD2c, and LSD1) at the translational level, and H3K9 trimethyltransferase (SUV39h1) at the post-translational level. The dysregulation of histone methyltransferases and demethylases is associated with the progression of several diseases, including cancer, and their inhibitors have already reached the first phases of clinical trials in cancer therapy (13, 25-27). Our findings indicated that CK2 could also be a valuable anticancer therapy target for regulating histone-modifying enzymes.

Our previous studies showed that p53 may be an important regulator in CK2 downregulation-mediated SAHF formation (22) and that CK2 downregulation may enhance the nuclear import of SUV39h1 by inhibiting the interaction between p53 and SUV39h1 (24). The present study showed that CK2 regulated the protein levels of JMJD2a, JMJD2c, and LSD1 in a p53-independent manner (Supplementary Fig. 2). However, the ectopic expression of JMJD2a and LSD1 suppressed the activation of p53 in CK2-downregulated cells, and the knockdown of JMJD2a and LSD1 abrogated the inactivation of p53 in CK2-upregulated cells (Fig. 3). Hence, these results indicated that JMJD2a and LSD1 are the upstream regulators of p53. In addition, histone lysine methyltransferases and demethylases have been reported to play significant roles in modifying p53 (14, 15). The present study showed that p53K370me2 expression was increased in CK2-downregulated cells and that the ectopic expression of JMJD2a or LSD1 suppressed this increase (Fig. 3A). These results suggest that the downregulation of JMJD2a and LSD1 increases the stability of p53 by preventing the removal of the methyl groups from p53K370me2 in CK2-downregulated cells.

The present study demonstrated the reduced coprecipitation of SUV39h1 with p53 in CK2-downregulated cells. The ectopic expression of JMJD2a or LSD1, however, enhanced the coprecipitation of SUV39h1 with p53 in these cells. In accordance, a greater amount of SUV39h1 was coprecipitated with p53 in cells with CK2α upregulation. However, the knockdown of JMJD2a or LSD1 inhibited the coprecipitation of SUV39h1 with p53 in these cells (Fig. 4A and B). In addition, the amount of SUV39h1 was higher in the nuclei than in the cytosol of cells with CK2 downregulation. The ectopic expression of JMJD2a or LSD1, however, suppressed the nuclear import of SUV39h1 in CK2-downregulated cells (Fig. 4C). Taken together, these results suggest that the CK2 downregulation-mediated reduction of JMJD2a and LSD1 stimulates the nuclear import of SUV39h1 by decreasing the interaction between p53 and SUV39h1. Previously, it was shown that the CK2 downregulation-induced dephosphorylation of S392 on p53 promoted H3K9me3 by inhibiting the interaction between p53 and SUV39h1, which resulted in the nuclear import of SUV39h1 (24). Therefore, our previous and present study findings suggest that CK2 regulates the nuclear import of SUV39h1 via two pathways: i) modulation of the p53S392 phosphorylation status by CK2 and ii) modulation of the p53K370 methylation status by JMJD2a and LSD1.

In conclusion, based on the present study results, we propose a model for the induction of H3K9me3 during CK2 downregulation-mediated senescence. The downregulation of CK2 may reduce the translation of JMJD2a and LSD1 by activating the mTOR–p70S6K pathway, thereby resulting in the accumulation of p53K370me2. In addition, the dimethylation of Lys370 on p53 may prevent the binding of p53 to SUV39h1, leading to the nuclear import of SUV39h1 and subsequently increased H3K9me3 (Fig. 4D).

MATERIALS AND METHODS

Materials

Antibodies against JMJD2a, LSD1, SUV39h1, histone H3, and H3K9me3 were purchased from Abcam (Cambridge, England), and antibodies against JMJD2c, CK2α, p53, $p21^{Cip1/WAF1}$, and β-actin were obtained from Santa Cruz Biotechnology (Santa Cruz, CA). Antibodies specific for phospho-mTOR (S2448) and phospho-p70S6K (T389) were obtained from Cell Signaling Technology (Beverly, MA), and anti-hemagglutinin (HA) antibody was obtained from Roche (Basel, Switzerland). Antibody against p53K370me2 was obtained from MyBioSource (San Diego, CA), and rhodamine-conjugated goat anti-rabbit IgG and DAPI were purchased from Invitrogen (Carlsbad, CA). 5-Bromo-4-chloro-3-indolyl-β-D-galactoside (X-gal), cycloheximide, and rapamycin were obtained from Sigma Chemical Co. (St. Louis, MO), and siRNAs for JMJD2a (sc-38463) and LSD1 (sc-60970) were purchased from Santa Cruz Biotechnology. The siRNA for CK2α was 5′-UCAAGAUGACUACCAGCUGdTdT-3′, and the siRNA for the negative control was 5′-GCUCAGAUCAAUACGGAGAdTdT-3′.

Cell culture and DNA transfection

Human colon cancer HCT116 cells (wild-type p53 and $p53^{-/-}$) and breast cancer MCF-7 and MDA-MB-435 cells (change of Gly to Glu at residue 266 on p53) were cultured in Dulbecco's modified Eagle's medium supplemented with 10% fetal bovine serum and 1% penicillin–streptomycin. pCMV-JMJD2a, pCMV-LSD1, pcDNA3.1-p53, and pcDNA3.1-HA-CK2α were transfected into cells using Polyfect (Invitrogen, CA) for 48 h. siRNAs were transfected into cells using Lipofectamine (Thermo Fisher Scientific, MA) for 48 h.

SA-β-gal activity assay

SA-β-gal activity was measured as described in a previous study (18).

Immunoblot and immunofluorescence analyses

Immunoblot analysis was performed as described in a previous study (19). Immunofluorescence analysis was performed using the anti-H3K9me3 (1:100) and HP1 (1:100) antibodies as described previously (22). DAPI was used to counterstain nuclei, and fluorescence signals were detected using Carl Zeiss Axioplan 2 microscope (Carl Zeiss, Jena, Germany). Fluorescence images were analyzed using ImageJ software (http://rsb.info.nih.gov/ij/).

Reverse transcription polymerase chain reaction (RT-PCR)

Total RNA was extracted from cells. RNA was reverse-transcribed using gene-specific primers and reverse transcriptase (Takara Bio Inc., Shiga, Japan), and the resulting cDNA was amplified using PCR. The primers used for the assays are listed in Supplemental Table 1. PCR products were resolved on a 1.5% agarose gel, and the RT-PCR bands were quantified using densitometry. Primers for β-actin RNA were used to standardize RNA levels in each sample.

Immunoprecipitation

Cell lysates were pre-cleared with normal mouse or rabbit IgG and protein A sepharose (Amersham Biosciences, GE Healthcare, Waukesha, WI) for 1 h at 4°C. The supernatant was

then incubated with anti-SUV39h1 or anti-p53 antibodies and protein A sepharose with mixing for 12 h at 4°C. The beads were then collected via centrifugation and washed three times with phosphate-buffered saline.

Isolation of nuclear and cytoplasmic extracts

According to the manufacturer's instruction, cytoplasmic and nuclear extracts were prepared using the NE-PER Nuclear Cytoplasmic Extraction Reagent kit (Pierce, Rockford, IL).

Statistical analysis

Data were analyzed using one-way analysis of variance in SPSS (IBM, Armonk, NY). The results were considered significant if the *P* value was <0.05. Duncan's multiple range test was performed if the differences between the groups were identified as $\alpha = 0.05$.

CONFLICT OF INTEREST

The authors declare no conflict of interest.

ACKNOWLEDGMENTS

This research was supported by the Basic Science Research Program through the National Research Foundation of Korea (NRF) funded by the Ministry of Science, ICT and Future Planning (NRF-2015R1A2A2A01004593 and NRF-2019R1A2C1005219).

REFERENCES

1. Campisi J (2013) Aging, cellular senescence, and cancer. Annu Rev Physiol 75, 685-705

2. Kuilman T, Michaloglou C, Mooi WJ and Peeper DS (2010) The essence of senescence. Genes Dev 24, 2463-2479

3. Dimri GP, Lee X, Basile G et al (1995) A biomarker that identifies senescent human cells in culture and in aging skin in vivo. Proc Natl Acad Sci U S A 92, 9363-9367

4. Zhang R, Chen W and Adams PD (2007) Molecular dissection of formation of senescence-associated heterochromatin foci. Mol Cell Biol 27, 2343-2358

5. Narita M, Nunez S, Heard E et al (2003) Rb-mediated heterochromatin formation and silencing of E2F target genes during cellular senescence. Cell 113, 703-716

6. Kouzarides T (2007) Chromatin modifications and their function. Cell 128, 693-705

7. Ait-Si-Ali S, Guasconi V, Fritsch L et al (2004) A Suv39h-dependent mechanism for silencing S-phase genes in differentiating but not in cycling cells. EMBO J 23, 605-615

8. Whetstine JR, Nottke A, Lan F et al (2006) Reversal of histone lysine trimethylation by the JMJD2 family of histone demethylases. Cell 125, 467-481

9. Couture JF, Collazo E, Ortiz-Tello PA et al (2007) Specificity and mechanism of JMJD2A, a trimethyllysine-specific histone demethylase. Nat Struct Mol Biol 14, 689-695

10. Gray SG, Iglesias AH, Lizcano F et al (2005) Functional characterization of JMJD2A, a histone deacetylase- and retinoblastoma-binding protein. J Biol Chem 280, 28507-28518

11. Shi Y, Lan F, Matson C et al (2004) Histone demethylation mediated by the nuclear amine oxidase homolog LSD1. Cell 119, 941-953

12. Wissmann M, Yin N, Muller JM et al (2007) Cooperative demethylation by JMJD2C and LSD1 promotes androgen receptor-dependent gene expression. Nat Cell Biol 9, 347-353

13. Berry WL and Janknecht R (2013) KDM4/JMJD2 histone demethylases: epigenetic regulators in cancer cells. Cancer Res 73, 2936-2942

14. Huang J, Sengupta R, Espejo AB et al (2007) p53 is regulated by the lysine demethylase LSD1. Nature 449, 105-108

15. Johmura Y, Sun J, Kitagawa K et al (2016) SCF(Fbxo22)-KDM4A targets methylated p53 for degradation and regulates senescence. Nat Commun 7, 10574

16. Wullschleger S, Loewith R and Hall MN (2006) TOR signaling in growth and metabolism. Cell 124, 471-484

17. Morita M, Gravel SP, Hulea L et al (2015) mTOR coordinates protein synthesis, mitochondrial activity and proliferation. Cell Cycle 14, 473-480

18. Ryu SW, Woo JH, Kim YH et al (2006) Downregulation of protein kinase CKII is associated with cellular senescence. FEBS Lett 580, 988-994

19. Kang JY, Kim JJ, Jang SY and Bae YS (2009) The p53-p21$^{Cip1/WAF1}$ pathway is necessary for cellular senescence induced by the inhibition of protein kinase CKII in human colon cancer cells. Mol Cells 28, 489-494

20. Park JH, Kim JJ and Bae YS (2013) Involvement of PI3K-AKT-mTOR pathway in protein kinase CKII inhibition-mediated senescence in human colon cancer cells. Biochem Biophys Res Commun 433, 420-425

21. Park JH, Lee JH, Park JW et al (2017) Downregulation of protein kinase CK2 activity induces age-related biomarkers in C. elegans. Oncotarget 8, 36950-36963

22. Park JW, Kim JJ and Bae YS (2018) CK2 downregulation induces senescence-associated heterochromatic foci formation through activating SUV39h1 and inactivating G9a. Biochem Biophys Res Commun 505, 67-73

23. Wei J, Ma L, Lai YH, et al (2019) Bazedoxifene as a novel GP130 inhibitor for colon cancer therapy. J Exp Clin Cancer Res 38, 63

24. Park JW and Bae YS (2019) Dephosphorylation of p53 Ser392 enhances trimethylation of histone H3 Lys9 via SUV39h1 stabilization in CK2 downregulation-mediated senescence. Mol Cells 42, 773-782

25. Morera L, Lubbert M and Jung M (2016) Targeting histone methyltransferases and demethylases in clinical trials for cancer therapy. Clin Epigenetics 8, 57

26. Monaghan L, Massett ME, Bunschoten RP et al (2019) The emerging role of H3K9me3 as a potential therapeutic target in acute myeloid leukemia. Front Oncol 9, 705

27. Fiskus W, Sharma S, Shah B et al (2014) Highly effective combination of LSD1 (KDM1A) antagonist and pan-histone deacetylase inhibitor against human AML cells. Leukemia 28, 2155-2164

28. Saramaki A, Banwell CM, Campbell MJ and Carlberg C (2006) Regulation of the human $p21^{waf1/cip1}$ gene promoter via multiple binding sites for p53 and the vitamin D3 receptor. Nucleic Acids Res 34, 543-554

Figure Legends

Fig. 1. Overexpression of JMJD2a and LSD1 suppresses CK2 knockdown-mediated SA-β-gal staining and SAHF formation. MCF-7 and HCT116 cells were treated with CK2α siRNA in the absence or presence of pCMV-JMJD2a and pCMV-LSD1. (A) Cells were stained with 5-bromo-4-chloro-3-indolyl-β-D-galactoside, and the percentage of blue-stained cells was determined. Values indicate the mean ± SEM. ***$P < 0.001$. (B) Confocal immunofluorescence images of the co-localization of chromatin foci with H3K9me3 (red) and HP1γ (green) in cells. DAPI staining (blue) was used to visualize DNA foci. The fluorescence intensity was quantified using ImageJ software (right panels). Arbitrary

intensity values for H3K9me3 (red), HP1γ (green), or DAPI (blue) are shown relative to the reference line (white) used for analysis.

Fig. 2. CK2 downregulation decreases the expression of JMJD2a and LSD1 at the translational level by activating the mTOR–p70S6K pathway. MCF-7 and HCT116 cells were transfected with (A) CK2α siRNA or pcDNA3.1-HA-CK2α, (B) CK2α siRNA in the presence of 50 μg/ml of cycloheximide (CHX) for the indicated times, or (C) CK2α siRNA or pcDNA3.1-HA-CK2α in the presence of 0.1 μM rapamycin. After 2 days, the level of each protein was determined via immunoblot analysis using antibodies against CK2α, hemagglutinin (HA, for HA-CK2α in Fig. 2A), JMJD2a, JMJD2c, LSD1, p-mTOR (S2448), and p70S6K (T389) (left panels). β-actin was used as a control. Graphs represent the quantification of each protein relative to β-actin (right panels). Data are shown as the mean ± SEM. *$P < 0.05$; **$P < 0.01$; ***$P < 0.001$. Bars that do not share a common letter (a, b, c, d) are significantly different among groups at $P < 0.05$.

Fig. 3. CK2 downregulation-mediated reduction of JMJD2a and LSD1 activates the p53–p21$^{Cip1/WAF1}$–SUV39h1–H3K9me3 axis. (A) Cells were treated with CK2α siRNA in the absence or presence of pCMV-JMJD2a and pCMV-LSD1. (B) Cells were treated with pcDNA3.1-HA-CK2α in the absence or presence of JMJD2a siRNA and LSD1siRNA. Cell lysates were visualized via immunoblotting (upper panels), and graphs represent the quantification of each protein relative to β-actin (bottom panels). Data are presented as the mean ± SEM. Bars that do not share a common letter (a, b, c) are significantly different among groups at $P < 0.05$.

Fig. 4. CK2 downregulation-mediated JMJD2a and LSD1 reduction stimulates the dimethylation of p53 Lys370 and leads to the nuclear import of SUV39h1. (A and C) Cells were treated with CK2α siRNA in the absence or presence of pCMV-JMJD2a and pCMV-LSD1. (B) Cells were treated with pcDNA3.1-HA-CK2α in the absence or presence of JMJD2a siRNA and LSD1siRNA. (A and B) Cell lysates were immunoprecipitated (IP) with anti-p53 antibodies, followed by immunoblotting with anti-SUV39h1 antibodies. The cell lysate IP with IgG heavy chain served as a loading control (upper panels). Representative data from three independent experiments are shown. Graphs represent the quantification of SUV39h1 relative to the heavy chain (bottom panels). (C) The cytoplasm and nuclei were isolated from cells, and both extracts were visualized via immunoblotting. β-actin (cytoplasmic marker) and histone H3 (nuclear marker) were used as loading controls (left panels). Graphs represent the quantification of p53K370me2, p53, and SUV39h1 relative to subcellular markers (right panels). Values indicate the mean ± SE. Bars that do not share a common letter (a, b, c) are significantly different among groups at $P < 0.05$. (D) Possible model illustrating the CK2 downregulation-mediated reduction of JMJD2a and LSD1 for SAHF formation.

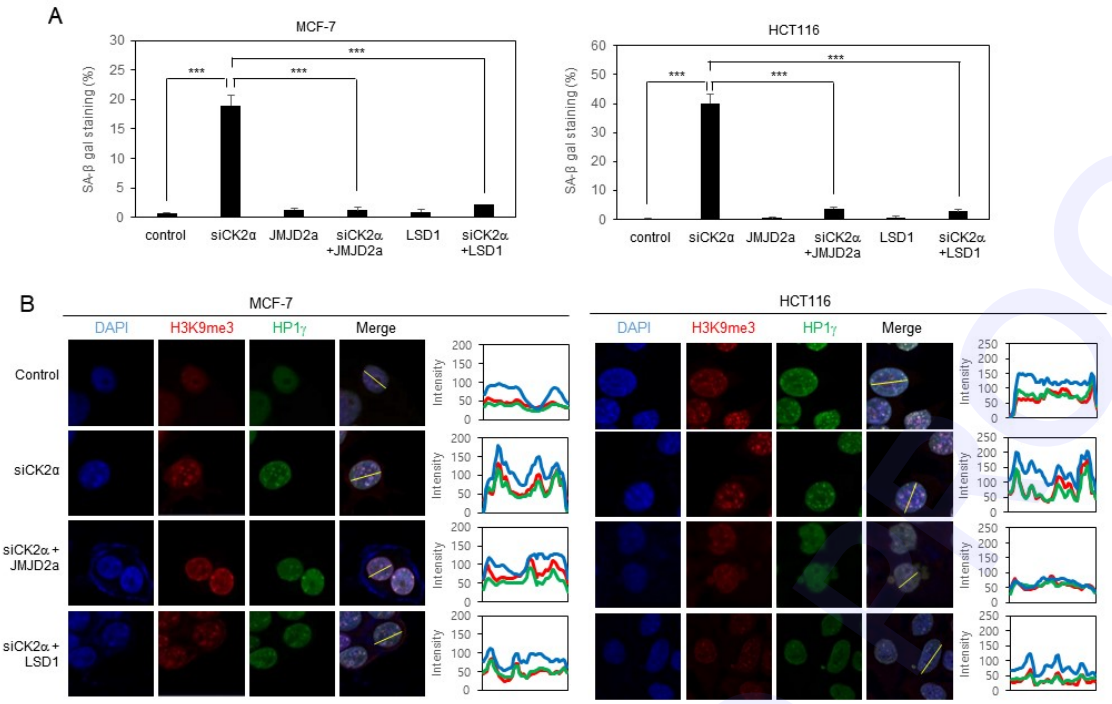

Fig. 1

Fig. 1. Fig. 1

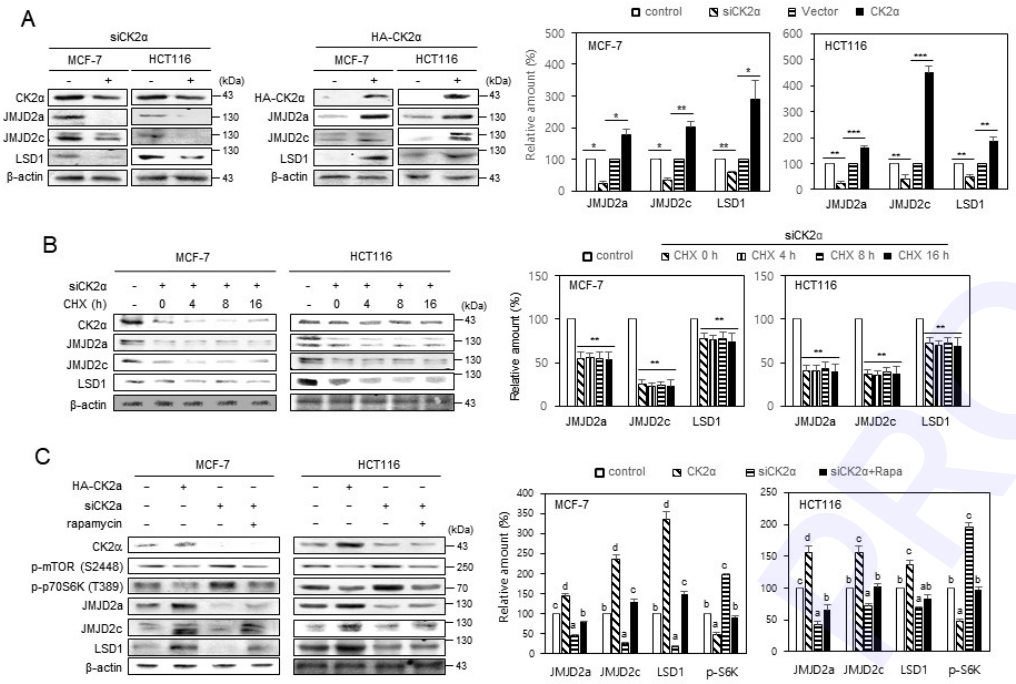

Fig. 2

Fig. 2. Fig. 2

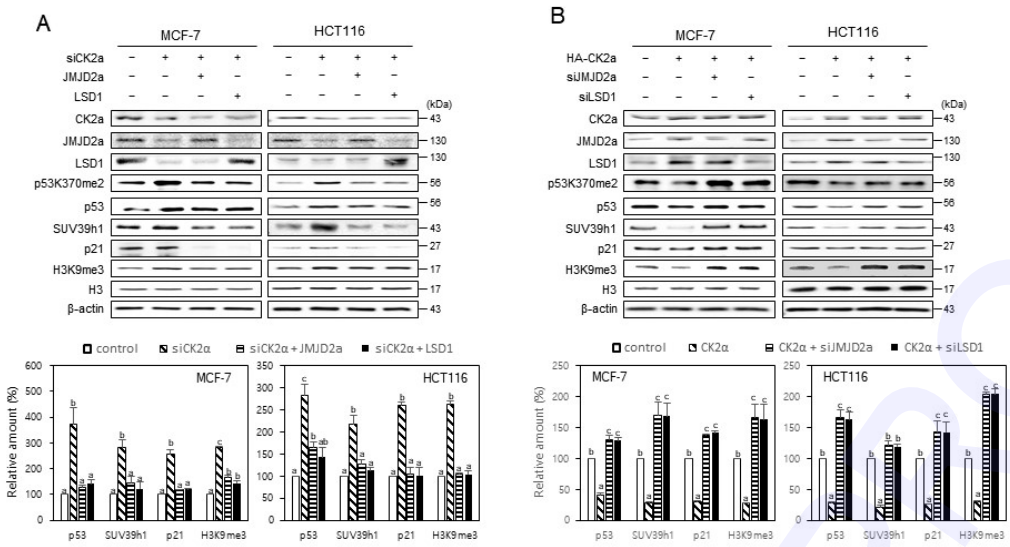

Fig. 3

Fig. 3. Fig. 3

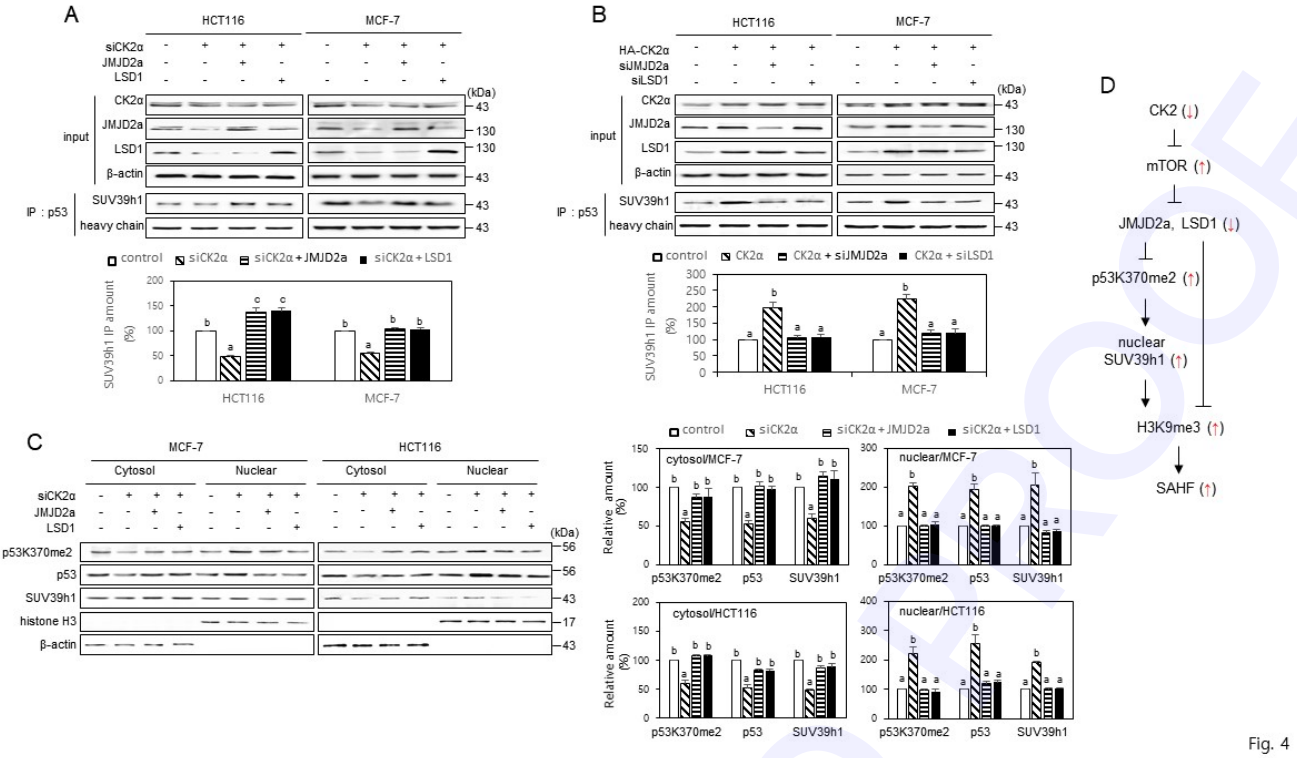

Fig. 4

Fig. 4. Fig. 4

Supplemental Materials and Methods

Colony formation assay

Cells were grown in 100 mm plates and transfected with siCK2α, LSD1, and JMJ2Da. After trypsinization, the viable cells were collected and seeded at 1000 cells per well in 60 mm dishes and allowed to grow until control cells reached confluence. Cells were washed with PBS twice and fixed with 4% paraformaldehyde for 10 min followed by staining with 1% crystal violet dye in 25% methanol at room temperature for 2 h. The plates were then rinsed with distilled water and dried before scanning.

Cell migration assay

When cells were 100% confluent, the monolayer was scratched to the same width using a yellow pipette tip. After 24 h culture, images were captured by using an inverted microscope (Nikon, Eclipse TS100, Japan). The percentage of wound-healing was measured by the ImageJ software (National Institutes of Health, USA) and calculated percent wound healing.

ChIP assay

ChIP assay with p53 antibody was performed as described previously (28). In addition, the DNA fragments were amplified with human $p21^{Cip1/WAF1}$ promoter primer pairs. Primer sequences used for assays were as follows: forward, 5'-CACCACTGAGCCTTCCTCAC-3' and reverse, 5' -CTGACTCCCAGCACACACTC-3'.

Supplemental Table 1. Primers used for RT-PCR analyses

Gene		Primer sequence
CK2α	Forward	5′-AAGACCCTGTGTCACGAACCC-3′
	Reverse	5′-GGCTCCTCCCGAAAGATCATAC-3′
JMJD2a	Forward	5′-GGTGCCATCCTCCTCAAGAT-3′
	Reverse	5′-AAGCAGAGGACCAAGCCATT-3′
JMJD2c	Forward	5′-ATTCTCCACCCAATGCCTTC-3′
	Reverse	5′-CTGCTGTCCACGCATTTCTT-3′
LSD1	Forward	5′-GCAGTCCAAAGGATGGGATT-3′
	Reverse	5′-AACATGCCCGAACAAATTGA-3′
β-actin (h)	Forward	5′-TCCCTGGAGAAGAGCTACGA-3′
	Reverse	5′-AGCACTGTGTTGGCGTACAG-3′

Supplemental figure legends

Supplementary Fig. 1. Overexpression of JMJD2a and LSD1 suppressed CK2 knockdown-mediated reduction of cancer cell colony-forming and migration abilities. MCF-7 and HCT116 cells were treated with CK2α siRNA in the absence or presence of pCMV-JMJD2a and pCMV-LSD1. (A) Cells were re-seeded at 1,000 cells per well and cultured to grow clones for three weeks. Cells were fixed with paraformaldehyde followed by staining with crystal violet dye. Representative pictures of colonies from three independent experiments are shown (top). The graphs represent the quantitation of colonies to the control (bottom). (B) Cell migration assay was conducted by scratching the cells with a yellow pipette tip when cells grew into a monolayer and then migrating into the scratched area for 24 h. The representative pictures show the cell migrating ability (left). Green arrows indicate a gap in the scratched area. The percentage of the migrating area was quantified. The graphs represent the quantitation of migrating area to the control (right). Values indicate the mean ± SE. Bars that do not share a common letter (a, b, c) are significantly different among groups at $P < 0.05$.

Supplementary Fig. 2. CK2 regulated JMJD2a and LSD1 expression in a p53-independent manner. HCT116 $p53^{-/-}$ and MDA-MB-435 cells were treated with CK2α siRNA or pcDNA3.1-CK2α, and cell extracts were visualized by immunoblotting using antibodies against CK2α, hemagglutinin (HA), JMJD2a, JMJD2c, and LSD1. β-actin was used as a control (upper panels). Graphs represent the quantification of each protein relative to β-actin (bottom panels). Data are shown as the mean ± SEM. $*P < 0.05$; $**P < 0.01$; $***P < 0 .001$.

Supplementary Fig. 3. CK2 regulated the expression of JMJD2a, JMJD2c, and LSD1 at the post-transcriptional level. MCF-7 and HCT116 cells were treated with CK2α siRNA or pcDNA3.1-HA-CK2α. Total RNA was extracted from the cells, and RT-PCR was performed using specific primers for genes coding CK2α, JMJD2a, JMJD2c, and LSD1. β-actin was used as a loading control (upper panels). Graphs represent the quantification of the mRNA level of each gene relative to that of β-actin (bottom panels).

Supplementary Fig. 4. Overexpression of JMJD2a and LSD1 suppressed CK2 knockdown-mediated reduction of p53 binding to *p21*$^{waf1/cip1}$ promoter. MCF-7 and HCT-116 cells were transfected with either CK2α siRNA in the presence of pCMV-JMJD2a or pCMV-LSD1 (A) or pcDNA3.1-HA-CK2α in the presence of JMJD2a siRNA or LSD1 siRNA (B) for 48h, ChIP assays using an anti-p53 antibody were performed. The interaction was determined by ChIP followed by real-time PCR using primers specific for *p21*$^{Cip1/WAF1}$. ChIP data were quantified using the comparative delta Cq values. Cq values resulting from cells were normalized both versus the input and subsequently versus no-antibody control. Graphs represent the quantification of *p21*$^{waf1/cip1}$ promoter region. Values indicate the mean ± SE. Bars that do not share a common letter (a, b, c) are significantly different among groups at $P < 0.05$.

Supplementary Fig. 5. Ectopic expression of p53 overcame SUV39h1 reduction mediated by overexpression of JMJD2a or LSD1 in CK2-downregulated cells. MCF-7 and HCT116 cells were treated with CK2α siRNA in the absence or presence of pCMV-JMJD2a, pCMV-LSD1, and pcDNA3.1-p53. Cell lysates were visualized by immunoblotting (upper panels), and graphs represent the quantification of each protein relative to β-actin

(bottom panels). Data are shown as the mean ± SEM. Bars that do not share a common letter (a, b, c) are significantly different among groups at $P < 0.05$.

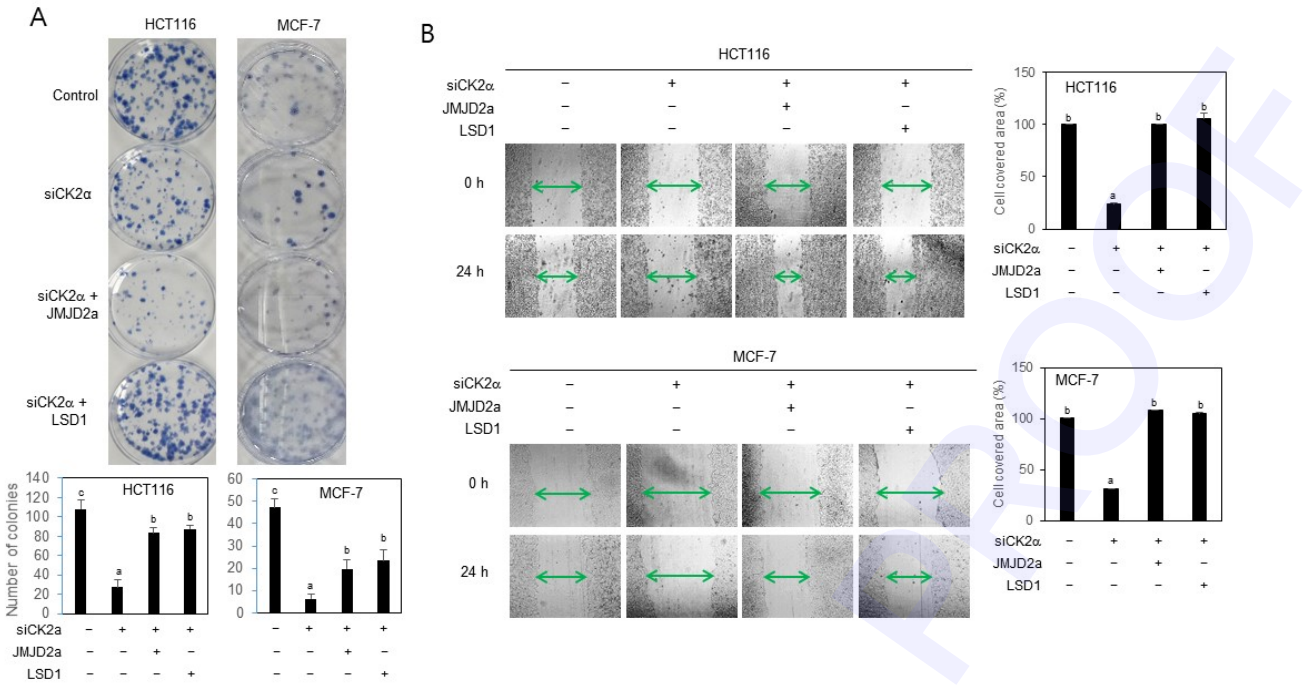

sFig. 1

Sup. 4.

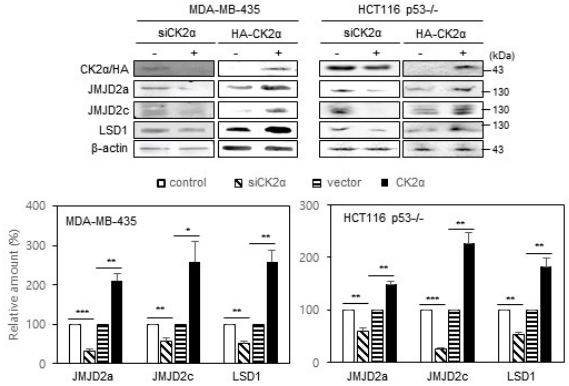

sFig. 2

Sup. 5.

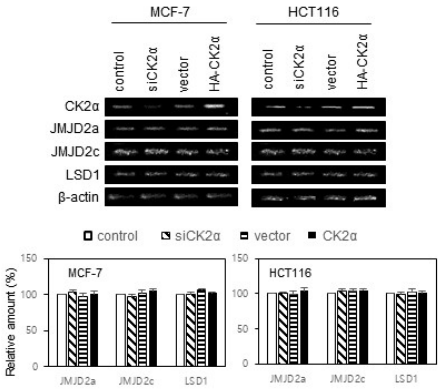

sFig. 3

Sup. 6.

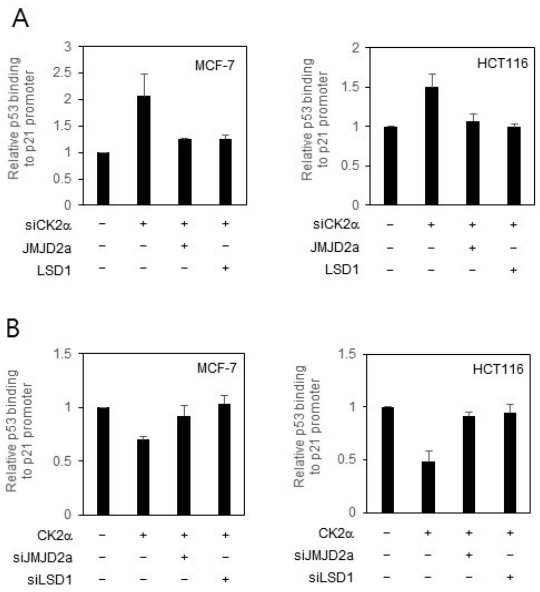

sFig. 4

Sup. 7.

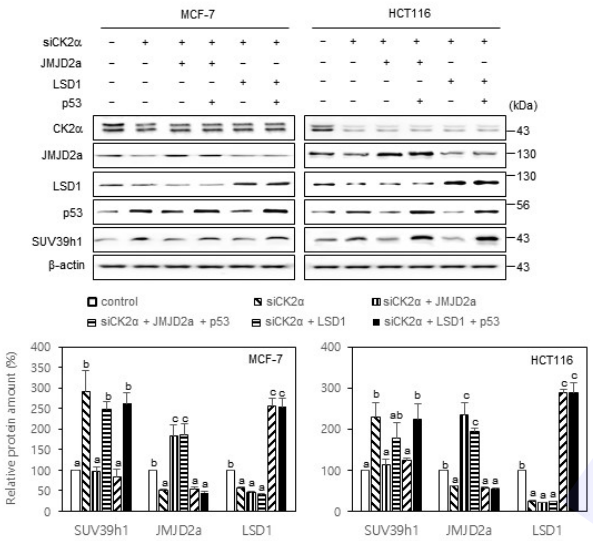

sFig. 5

Sup. 8.